Mechatronic Systems 2

Applications in Material Handling Processes and Robotics

Edited by
Leonid Polishchuk
Orken Mamyrbayev
Konrad Gromaszek

ROUTLEDGE

Mechatronic Systems 2

Mechatronic Systems 2

Applications in Material Handling Processes and Robotics

Edited by

Leonid Polishchuk
Vinnytsia National Technical University, Vinnytsia, Ukraine

Orken Mamyrbayev
Institute of Information and Computational Technologies CS MES RK, Almaty, Kazakhstan

Konrad Gromaszek
Lublin University of Technology, Lublin, Poland

Routledge
Taylor & Francis Group
LONDON AND NEW YORK

Cover image: Andrzej Kotyra
First published 2021
by Routledge/Balkema
Schipholweg 107C, 2316 XC Leiden, The Netherlands
e-mail: enquiries@taylorandfrancis.com
www.routledge.com – www.taylorandfrancis.com

Routledge/Balkema is an imprint of the Taylor & Francis Group, an informa business

© 2021 selection and editorial matter, Leonid Polishchuk, Orken Mamyrbayev, Konrad Gromaszek; individual chapters, the contributors

The right of Leonid Polishchuk, Orken Mamyrbayev, Konrad Gromaszek to be identified as the authors of the editorial material, and of the authors for their individual chapters, has been asserted in accordance with sections 77 and 78 of the Copyright, Designs and Patents Act 1988.

All rights reserved. No part of this book may be reprinted or reproduced or utilized in any form or by any electronic, mechanical, or other means, now known or hereafter invented, including photocopying and recording, or in any information storage or retrieval system, without permission in writing from the publishers.

Although all care is taken to ensure integrity and the quality of this publication and the information herein, no responsibility is assumed by the publishers nor the author for any damage to the property or persons as a result of operation or use of this publication and/or the information contained herein.

Library of Congress Cataloging-in-Publication Data
A catalog record has been requested for this book

ISBN: 978-1-032-10585-7 (Hbk)
ISBN: 978-1-032-12621-0 (Pbk)
ISBN: 978-1-003-22544-7 (eBook)

DOI: 10.1201/9781003225447

Typeset in Times New Roman
by codeMantra

Contents

Chapter 1

Development of perspective equipment for the regeneration of industrial filters

I. Sevostyanov, I. Zozulyak, Y. Ivanchuk, O. Polischuk, K. Koval, W. Wójcik, A. Kalizhanova, and A. Kozbakova

CONTENTS

1.1 INTRODUCTION

The problem of the lack of clean drinking water is becoming urgent for an increasing number of regions in different countries, especially in large cities with high levels of environmental pollution and in industrial zones. Quality water is a determining factor for the food and chemical industry, pharmacology, microbiology, and microelectronics. In addition, in Europe, including Belarus, Russia, and the Ukraine, there are quite a few areas with high natural hardness of water. In this regard, industrial and household filters and filter systems are increasingly being used.

One of the main stages of high-quality water purification is its degreasing and softening. In most cases, they are implemented using ion-exchange resin cartridge filters as filter fillers. However, in the process of using such filters, when cleaning sufficiently hard water, they lose their performance within a year. It should be added that the majority of enterprises and private users of these filters are interested in their regeneration. The latter is carried out using a 10% solution of salt. The regenerated resin is soaked in the salt solution for 8–10 hours. At the same time, for sufficiently high-quality recovery, it is necessary to ensure periodic mixing of the resin in the salt solution with a velocity of $v_{\min} = 0.01$ m/s. This is needed to penetrate into the lower layers of the portion of consumables. However, this is not always done, and therefore, regeneration is incomplete, and the life of such cartridges will be limited. Further, it is necessary to consider the viscosity of the mixed material. According to our experimental data, it is $\mu_m = 1.32$–1.38 Pa/s, as well as the true resin density of $\rho_m = 1.04 \cdot 10^{-3}$ kg/m^3.

Thus, the actual task is the selection or development of equipment for the effective mixing of ion-exchange resin in saline solution. This equipment should be compact, reliable, inexpensive, and convenient in operation.

DOI: 10.1201/9781003225447-1

1.2 ANALYSIS OF LITERATURE DATA AND PROBLEM STATEMENT

From the known equipment, the most suitable are the agitators and mixers for wet dispersed materials. They are used in construction and in the food industry. Mixers and mixers for food production are divided into (Dragilev & Drozdov, 1999; Saravacos, 2002) high-speed and low-speed, uninterrupted, and periodic action, with stationary fixed and nonstationary chambers with screw, vane, rotor, anchor, propeller, turbine, drum, and finger actuators, providing radial, axial, or radial–axial flows of a stirred medium. Taking into account the above conditions and requirements for equipment for mixing ion-exchange resin in saline solution, batch mixers with a stationary fixed chamber and a radial–axial flow of the mixed solution are most suitable. Then, in accordance with the diagram given in (Dragilev & Drozdov, 1999), it is necessary to use propeller turbines with flat blades, paddle, or frame mixers, and mixers for mixing materials with the above viscosity (Bartholomai, 1987, Hakansson et al., 2016a, b).

Figure 1.1 shows the scheme of the predeterminer PR-3 with a turbine agitator (Dragilev & Drozdov, 1999). It is used in sugar beet production, the executive elements of which are the blades (9, 12, and 13), mounted on a shaft (8), driven in rotation by an electric motor (7). In this case, the blades (9) are designed to remove foam in the duct (5), and mixing the product coming through the nozzle (4) provides the blades (12). The blades (13) serve to prevent congestion when removing the product for unloading through the nozzle at the bottom of the pre-defector. The mixing process is also facilitated by counter-patches (11), mounted on the inner surface of the housing (10). In our opinion, the mixing process is effectively carried out only in the lower central part of this unit, while the upper and peripheral layers are less affected. In addition, the circulation and return of the product to the zone of more intensive mixing are not ensured. With a shaft rotation frequency of 8 $n = 64\,\mathrm{min}^{-1}$ and a case diameter of 10 $D = 2.4\,\mathrm{m}$ (Dragilev & Drozdov, 1999), the average linear velocity of the product being mixed is shown in equation (1.1):

$$v_n = \frac{\pi \cdot n}{30}\frac{D}{2} = \frac{3.14 \cdot 64 \cdot 1.2}{30 \cdot 2} \approx 4\,\mathrm{m/s} \tag{1.1}$$

which is significantly higher than $v_{\min}$ and in accordance with the formula for determining the power of rotation of the shaft (8), shown in equation (1.2):

$$N_n = F_c v_n, \tag{1.2}$$

in which F_c is the strength of resistance to mixing. It depends mainly on the processed product and leads to a corresponding unnecessary increase in energy consumption for mixing (the nominal power of the electric motor of the predeterminer PR-3 is $N_{\mathrm{nom}} = 13\,\mathrm{kW}$).

Figure 1.2 shows a homogenizer with a paddle stirrer (5) (Dragilev & Drozdov, 1999). It is driven from the electric motor (9), through the V-belt transmission (8) and the shaft (6). The product is fed through the nozzle (7), mixed in the hopper (4), and discharged through the nozzle (1). This device is designed for quick mixing of the product, which in continuous flow passes through the hopper (4). In this regard, the latter has a relatively small capacity. This circumstance does not allow for the use of

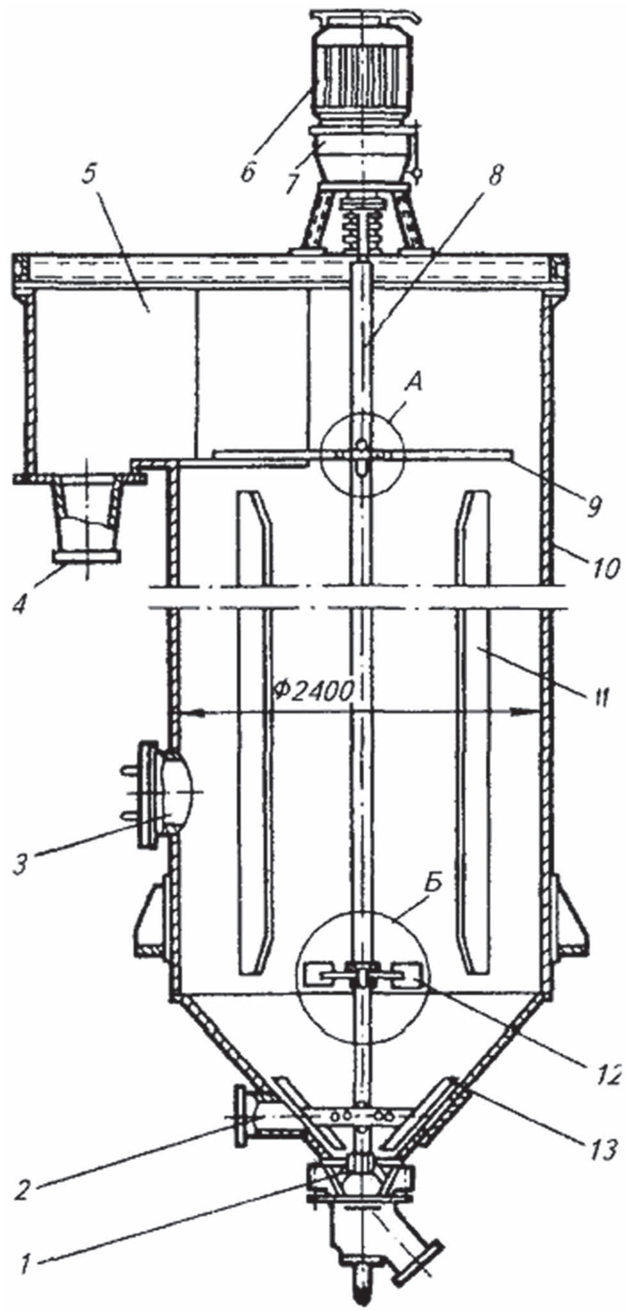

Figure 1.1 Scheme of predeterminer PR-3: (1) bearing; (2) inlet fitting; (3) access hatch; (4) outlet; (5) foam box; (6) electric motor; (7) gearbox; (8) vertical shaft; (9, 12, 13) mixers; (10) the case; (11) counterfeit.

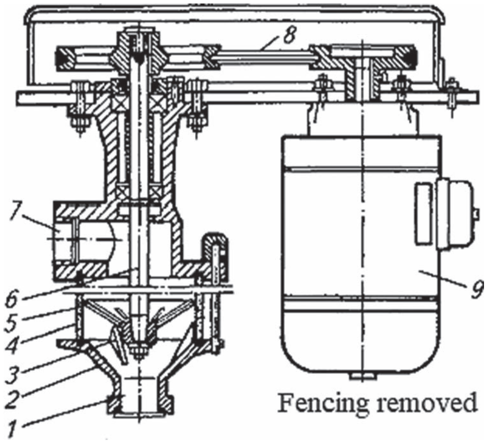

Figure 1.2 Scheme of the homogenizer: (1) outlet; (2) bottom; (3) ledge; (4) housing; (5) stirrer; (6) vertical shaft; (7) inlet; (8) V-belt transmission; (9) electric motor.

a homogenizer for long-term mixing of sufficiently large portions of the ion-exchange resin with a salt solution (Concidine, 2012).

The frequency of rotation of the shaft (6) of the homogenizer is $n = 950\,\text{min}^{-1}$, and the diameter of the body 4 is $D = 0.16\,\text{m}$ (Dragilev & Drozdov, 1999). Then, in accordance with the formula (1), the average linear velocity of the stirred product is:

$$v_n = \frac{\pi \cdot n}{30}\frac{D}{2} = \frac{3.14 \cdot 950 \cdot 0.08}{30 \cdot 2} = 3.97\,\text{m/s},$$

which also leads to unnecessary energy consumption (see formula (equation 1.2). The nominal power of the motor homogenizer is $N_{\text{nom}} = 0.28\,\text{kW}$ (Dragilev & Drozdov, 1999).

MT-250 machines for mixing and tempering various viscous masses, kneading machines with horizontal shafts, and a horizontal DÜC-C con-machine are also complicated, constructive, non-technological in manufacturing, expensive, and excessively powerful (Dragilev & Drozdov, 1999; Sevostyanov, 2013). The design of the kneading machine TM-63M (Dragilev & Drozdov, 1999) provides for the continuous passage of the processed material through it. In addition, the Z-shaped blades of the machine, performing the function of actuating elements, are rather non-technological.

The bubbler (Sevostyanov et al., 2015) shown in Figure 1.3 is a pneumatic-type agitator. Compressed air is fed into its tank, which is filled with the material being processed, through a tube or a system of tubes with small holes. Pop-up bubbles of the latter capture and mix material particles. However, as noted in (Geissler et al., 2014; Sevostyanov et al., 2015), pneumatic mixing is much less energy efficient than mechanical.

The most consistent with the above requirements and conditions is the mixer SMKN (Hakansson et al., 2016a, b) (Figure 1.4). It consists of two horizontal shafts (6), equipped with figured blades (5), deployed relative to the axes of the shafts at 60 degrees. This arrangement of the blades and the presence of holes in them ensure

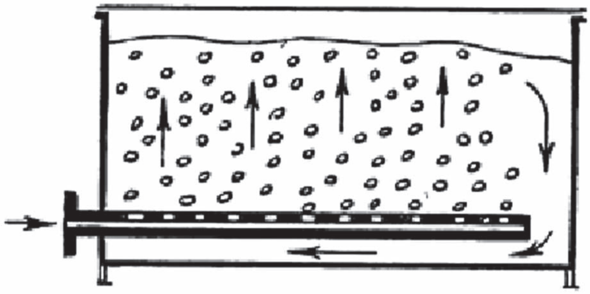

Figure 1.3 Diagram of the bubbler.

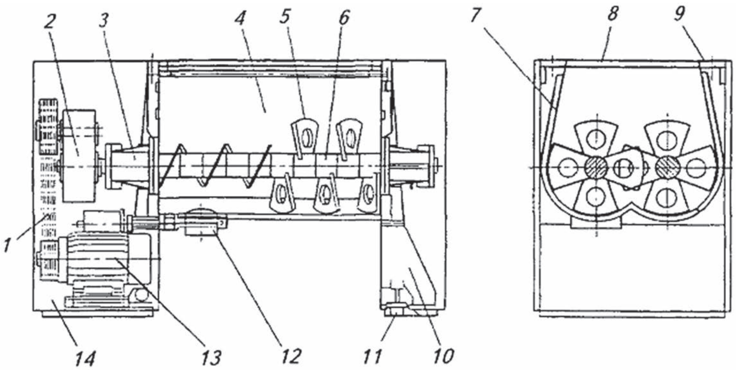

Figure 1.4 Mixer circuit SMKN: (1) V-belt transmission; (2) gearbox; (3) shaft support; (4) working chamber; (5) the blade; (6) shaft; (7) shirt; (8) lattice; (9) cover; (10) bed; (11) sensor; (12) inlet; (13) electric motor; (14) drive housing.

effective mixing of the product with its oncoming movement along the walls of the housing (4). The shaft (6) is driven from the electric motor (13) through the V-belt drive (1) and the gearbox (2). However, the mixer contains a shirt (7) that is not needed for regeneration of the resin. It is filled with paraffin oil with electric heaters. Taking into account the speed of rotation of the shafts (6) – $n = 38\,\text{min}^{-1}$ and the diameter of the blades (5) – $D = 0.9\,\text{m}$ by the formula (equation 1.1), we find that the average velocity of the particles of the mixed product provided by the mixer equals 0.89 m/s:

$$v_n = \frac{\pi \cdot n}{30}\frac{D}{2} = \frac{3.14 \cdot 38 \cdot 0.45}{30 \cdot 2} = 0.89\,\text{m/s},$$

This is noticeably more $v_{\min} = 0.01\,\text{m/s}$ and allows us to conclude that the mixer has insufficient energy efficiency. The nominal power of the mixer motor is $N_{\text{nom}} = 55\,\text{kW}$ (Hakansson et al., 2016a, b).

In accordance with the results of the above analysis, it is obvious that the available serial machines for mixing dispersed masses do not satisfy the basic requirements for the regeneration equipment of ion-exchange resin.

During the operation, they must ensure uniform continuous circulation of ion-exchange resin with a dynamic viscosity $\mu_{m=}1.38$ Pa/s in the working chamber with a speed of $v_{\min} = 0.01$ m/s. In addition, they should have a simple and reliable design, created based on proven components of known equipment.

To achieve this goal, it is necessary to solve the following main tasks:

1. To eliminate the abovementioned disadvantages of the known equipment for mixing wet dispersed materials to optimize their design in terms of the power and speed of mixing.
2. Develop dependencies to determine the basic operating parameters of the proposed equipment, including the power and speed of mixing, necessary for the subsequent development of the methodology for its design calculation.

1.3 MATERIALS AND RESEARCH METHODS

As starting materials for solving the formulated tasks, we use the above schemes of the known equipment for mixing wet dispersed materials. We also use the identified deficiencies of the known equipment and formulas to take into account their specific requirements to determine their main operating parameters.

The dependencies of mechanics, hydraulics, and the theory of vibro-impact machines were used as a method for deriving dependencies to calculate the optimal operating parameters of the proposed equipment.

1.4 DEVELOPMENT OF EQUIPMENT FOR THE REGENERATION OF ION-EXCHANGE RESIN

Figure 1.5 shows a diagram of a twin-screw agitator, in which the electric motor (1), through the planetary gearbox (2) and the open gear transmission (3), rotates the screws (4) and (5) located in the hopper (6). Resin and salt solution is also loaded into the bunker for regeneration. Due to the opposite direction of the turns of the screws 4 and 5, rotating in one and the same direction, a circular movement of the processed material along the walls of the bunker is ensured, not only in the longitudinal direction but also in the transverse direction. Thereby, conditions are created for maximum mobility of the resin particles, penetration of the regenerating solution between them, and their intensive recovery (Zhu et al., 2016).

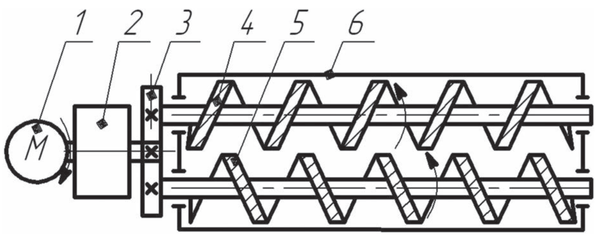

Figure 1.5 Diagram of a twin-screw mixer: (1) electric motor; (2) gearbox; (3) open gear; (4, 5) screws; (6) bunker.

The required drive power of the screws (4) and (5) of the mixer is determined by formula (Obertyukh et al., 2019):

$$N_n = 2 \cdot g \cdot Q_{\max} L_{\mathrm{sc}} \omega \cdot k_z \cdot 10^{-3} \tag{1.3}$$

where $Q_{\max}$ is the maximum performance of the mixer; L_{sc} is the length of the mixing screw, m ($L_{\mathrm{sc}} = 2.2 \div 2.5\,\mathrm{m}$); ω is the coefficient of resistance to movement ($\omega = 4 \div 5$); k_z is the power safety factor ($k_z = 1.2 \div 1.25$).

Performance can be determined by taking into account the required minimum of movement speed for the processed material in the axial direction $v = 0.01\,\mathrm{m/s}$, cross-sectional area S_m of the flow of the material in one direction, and its density ρ_m shown in the formula (equation 1.4):

$$Q_{\max} = \frac{S_m \cdot v}{2 \cdot \rho_m} \tag{1.4}$$

Substituting formula (equation 1.4) into formula (equation 1.3), we obtain:

$$\begin{aligned} N_n &= \frac{g \cdot S_m \cdot v \cdot L_{sc} \cdot \omega \cdot k_z \cdot 10^{-3}}{\rho_m} = \frac{g \cdot \pi \cdot D_m^2 \cdot v \cdot L_{sc} \cdot \omega \cdot k_z \cdot 10^{-3}}{4 \cdot \rho_m} \\ &= \frac{9.81 \cdot 3.14 \cdot 0.4^2 \cdot 0.01 \cdot 2.5 \cdot 5 \cdot 1.25 \cdot 10^{-3}}{4 \cdot 1.01 \cdot 10^{-3}} = 0.185\,\mathrm{kW} \end{aligned} \tag{1.5}$$

On the basis of N_n, the power of the auger drive motor can be determined by the formula (equation 1.6):

$$N_{dm} = \frac{N_n}{\eta_{dsc}} = \frac{N_n}{\eta_c \eta_g \eta_{og} \eta_{gr}} = \frac{0.185}{0.98 \cdot 0.75 \cdot 0.94 \cdot 0.99 \cdot 0.99} = 0.273\,\mathrm{kW} \tag{1.6}$$

where η_{dsc}, η_c, η_g, η_{og}, η_{gr} are the efficiency of the augers drive, the coupling between the electric motor (1) and the gearbox (2) (not shown in Figure 1.1), the gearbox (2), the open gear train (3), and the bearings in which the screws are mounted, respectively.

As can be seen, the obtained value is significantly less than most types of known equipment of similar purpose, discussed above. At the same time, only the homogenizer (Figure 1.2) has a proportional power. However, this does not provide the necessary processing time for a portion of the resin.

Figure 1.6 shows a diagram of a centrifugal agitator. A portion of the processed material is loaded into it through the hatch (5), after which the rotation of the impeller (1) with blades (2) is activated. They ensure the material is pumped in the direction shown by arrows from the center of the wheel to the channel (3) and further along pipe (6) back to the center. As a result, there is intensive mixing and regeneration of the material.

In accordance with (Iskovich-Lototsky et al., 2019), the flow rate of a centrifugal pump, the analogue, which is this mixer, is determined by the formula (equation 1.7):

$$Q = 2 \cdot \pi \cdot R \cdot b \cdot \psi \cdot \eta_0 \cdot v_m, \tag{1.7}$$

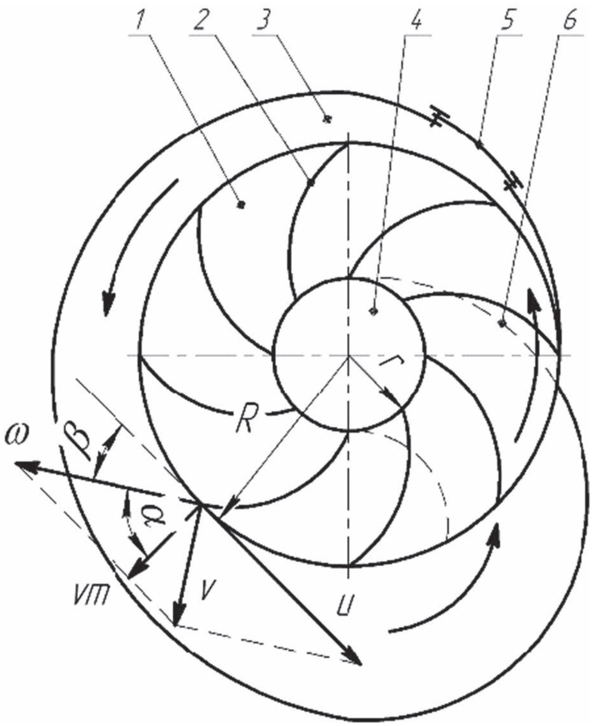

Figure 1.6 Centrifugal agitator: 1 impeller; (2) scapula; (3) channel; (4) inlet; (5) exit hatch; (6) return pipe.

where R is the radius of the impeller 1; b is the width of the impeller at the output; ψ is the compression ratio at the exit of the impeller; η_o is the volumetric efficiency; and v_m is the meridian component of the absolute velocity of the material v at the output.

The coefficient ψ was found according to the empirical formula (equation 1.8) (Iskovich-Lototsky et al., 2019):

$$\psi = 1 - \frac{z \cdot \delta}{2 \cdot \pi \cdot R \cdot \sin\beta}, \tag{1.8}$$

where z is the number of blades; δ is the blade thickness.

Actual head H is provided by the agitator formula (equation 1.9) (Franceschinis et al., 2014):

$$H = \frac{u \cdot v \cdot \cos\alpha}{g} \eta_{mx} k_z, \tag{1.9}$$

where u is the speed of the portable movement of the material; η_{mx} is the hydraulic efficiency of the mixer; k_z is the dimensionless coefficient of influence of a finite number of stirrer blades, determined by the following formula (equation 1.10) (Iskovich-Lototsky et al., 2019):

$$k_z = \frac{1}{1 + \frac{2 \cdot \varphi}{z\left[1 - \left(r/R\right)^2\right]}}, \tag{1.10}$$

where φ is the coefficient taking into account the influence of the guide vane ($\varphi = 0.8$–1.0- in the presence of the guide vane, $\varphi = 1.0$–1.3- in its absence); r is the radius of the inner edges of the blades.

The shaft power of the agitator formula (equation 1.11) is defined as:

$$N_n = \frac{Q \cdot \rho \cdot g \cdot H}{\eta}, \tag{1.11}$$

where ρ is the density of the material being processed; η is the overall efficiency of the mixer.

To calculate the estimated value of N_n taken, $v_m = v_{\min} = 0.01$ m/s. Then with such a low speed of the material, the impeller head H can be calculated based on atmospheric pressure as shown in equation (X):

$$H = \frac{p_a}{\rho_m \cdot g} = \frac{101{,}300}{1.04 \cdot 10^{-3} \cdot 9.8} = 9.9 \cdot 10^6 \,\text{m},$$

and the compression of the material at the exit of the impeller is neglected ($\psi = 1$). Then by the formulas (equation 1.7) and (equation 1.11), we get:

$$\begin{aligned} N_n &= \frac{2 \cdot \pi \cdot R \cdot b \cdot \psi \cdot \eta_o \cdot v_{\min} \cdot \rho_m \cdot g \cdot H}{\eta} \\ &= \frac{2 \cdot 3.14 \cdot 0.25 \cdot 0.05 \cdot 1 \cdot 0.9 \cdot 0.01 \cdot 1.04 \cdot 10^{-3} \cdot 9.81 \cdot 9.9 \cdot 10^6}{0.6} \\ &= 1{,}189 \approx 1.2\,\text{kW}. \end{aligned}$$

The resulting power value is also quite small. Figure 1.7 shows a drum mixer with work surfaces tilted at different angles. The principle of operation of the concrete mixer and the drum screen was described by Morgano et al. (Morgano et al., 2015). After loading a portion of the processed material (4) into the drum (3), the electric motor (1) is turned on, which, through the gearbox (2), causes the drum to rotate. As a result, the material in the drum interacts with work surfaces tilted at different angles. This contributes to its better mixing and recovery (Muschiolik & Dickinson, 2017).

The maximum torque of the drum formula (equation 1.12) is defined as:

$$M = m \cdot g \cdot r \tag{1.12}$$

where m is the portion's mass of the processed material, and r is the radius of the center of the portion mass (see Figure 1.7).

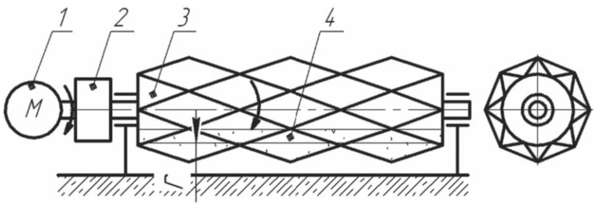

Figure 1.7 Diagram of a drum mixer with working surfaces tilted at different angles: (1) electric motor; (2) gearbox; (3) drum; (4) processed material.

The necessary power for mixing is calculated by the following formula (equation 1.13),

$$N_n = M \cdot \omega = M \frac{v}{r} \tag{1.13}$$

where ω and v are the minimum angular frequency and speed necessary for mixing and effective recovery of the material being processed, respectively (Obertyukh et al., 2018).

Then, after substituting formula equation (1.12) into formula equation (1.13), we obtain the following formula (equation 1.14):

$$N_n = m \cdot g \cdot v \tag{1.14}$$

The optimum drum speed (equation 1.15) can be calculated as:

$$n = \frac{2 \cdot v}{\pi \cdot r} \tag{1.15}$$

The mass m is determined based on the approximate dimensions of the drum (3) and the density ρ_m using the formula below:

$$m = \frac{\pi \cdot D_b^2}{8} L_b \cdot \rho_m = \frac{3.14 \cdot 0.7^2}{8} \cdot 2 \cdot 1.04 \cdot 10^{-3} 0.01 = 4 \cdot 10^{-6} \text{kg}$$

Then, in accordance with formula equation (1.14), we obtain $N_n = 4 \cdot 10^{-6} \cdot 9.81 \cdot 0.01 = 3.92 \cdot 10^{-10}$ kW, which is negligible power.

Figure 1.8 shows a structurally simpler scheme compared with the previous mixer. After loading a portion of the processed material (5) into the drum (3), its rotation is activated, which is provided by the electric motor (1) by means of the reducer (2). When the drum rotates, the blades (4) attached to its inner surface ensure that the material is mixed. To determine the required mixing power, formulas (equations 1.12–1.15) can be used.

The mixer with unbalance vibrators (Figure 1.9) provides more intensive and dynamic mixing of the portion of the processed material (2) in the container (1). Vibrators (3) are unbalanced with drives from the electric motors, during the rotation of which vertical power pulses are transmitted to the container (2) alternately up and then down (Polishchuk et al., 2016). As a result, the container, mounted on the springs (4), makes periodic vertical reciprocating movements (Kozlov et al., 2019, Polishchuk & Kozlov, 2018; Polishchuk et al., 2019).

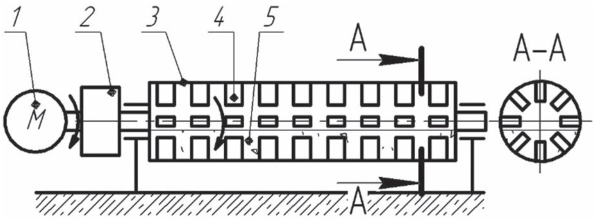

Figure 1.8 Diagram of a drum mixer with straight blades: (1) electric motor; (2) gearbox; (3) drum; (4) blades; (5) processed material.

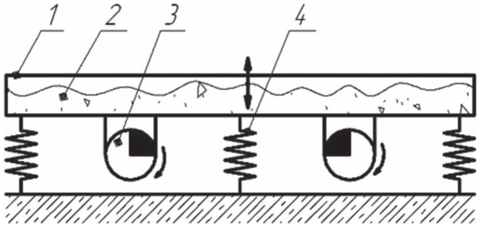

Each container movement cycle can be divided into four stages (Iskovich-Lototsky et al., 2019):

Stage I: Moving the container from its lowest position up to the middle position with fully compressed springs. This position is characterized by the absence of deformation of the springs.
Stage II: Moving the container further up from the middle to the highest position before stopping and stretching the springs.
Stage III: Moving the container from the top to the middle position.
Stage IV: Moving the container from the middle to the lowest position.

The motion equations of the container at each of these stages are:

For Stage I (equation 1.16):

$$M \cdot \ddot{z} = \frac{m \cdot v^2}{r} k + c \cdot l \cdot \left(\frac{A}{2} - z \right) - M \cdot g; \quad 0 \le z \le \frac{A}{2}; \quad 0 \le t \le \frac{15}{n} \tag{1.16}$$

For Stage II (equation 1.17):

$$-M \cdot \ddot{z} = \frac{m \cdot v^2}{r} k - c \cdot l \cdot z - M \cdot g; \quad 0 \le z \le \frac{A}{2}; \quad \frac{15}{n} < t \le \frac{30}{n} \tag{1.17}$$

For Stage III (equation 1.18):

$$-M \cdot \ddot{z} = -\frac{m \cdot v^2}{r} k - c \cdot l \cdot \left(\frac{A}{2} - z \right) - M \cdot g; \quad 0 \le z \le \frac{A}{2}; \quad \frac{30}{n} < t \le \frac{45}{n} \tag{1.18}$$

For Stage IV (equation 1.19):

$$M \cdot \ddot{z} = -\frac{m \cdot v^2}{r} k + c \cdot l \cdot z - M \cdot g; \quad 0 \le z \le \frac{A}{2}; \quad \frac{45}{n} < t \le \frac{60}{n} \tag{1.19}$$

Where M is the mass of the container with a portion of material (2) and vibrators (3); z is movement of the container; m is the unbalance mass of the vibrator (3); v is the angular velocity of rotation of the unbalance, which is selected in accordance with the minimum speed required for the material regeneration process; r is the radius of the center of the unbalanced mass of the vibrator relative to its axis of rotation; k is the number of vibrators; c is the stiffness coefficient of the spring (4); l is the number of springs; A is the amplitude of oscillation of the container; n is the rotational speed of the unbalance, and m/min; t is a time.

From the analysis of equations (1.13) through (1.15), it is obvious that the greatest value of the driving force is necessary at the end of Stage I at $z = A/2$; $t = 15/n$ (see equation (1.15). Then the corresponding mixing power can be found from equation (1.20):

$$N_n = F_{\max} v = \frac{m \cdot v^3}{r} k = \frac{1 \cdot 0.01^3}{0.1} 2 = 2 \cdot 10^{-7} \, \text{kW} \tag{1.20}$$

This power is also insignificant compared with the power of the known equipment.

1.5 CONCLUSION

The available equipment that can be used to mix the ion-exchange resin in saline solution is, in most cases, complex and low-tech to manufacture. It often does not ensure uniform mixing of the entire mass of the resin being restored and its circulation in the working chamber, which is of great importance for the quality of the recovery of the resin.

This chapter proposed ideas for special equipment for the regeneration of ion-exchange resin. In accordance with the calculations given, it provides, in comparison with the known equipment, a reduction in the required power of the driving motor by 1.5–48 times and the speed of mixing of the processed material, which is 90–400 times. This provides a corresponding reduction in energy consumption for the implementation of the workflow and an increase in its efficiency.

The dependencies for determining the basic operating parameters of the proposed equipment are given. These dependencies allow one to choose the most rational option and the methodology whereby the design calculation is created.

REFERENCES

Bartholomai, A. 1987. *Food Factories: Processes, Equipment, Costs*. Weinheim: VCH.

Concidine, D.M. 2012. *Foods and Food Production Encyclopedia*. Springer Science & Business Media, USA, 2301 p.

Dragilev, A.I., & Drozdov, V.S. 1999. *Technological Machines of Food Production*. Moscow: Kolos.

Franceschinis, E., Santomaso, A.C., Trotter, A., & Realdon, N. 2014. High shear mixer granulation using food grade binders with different thickening power. *Food Research International* 64: 711–717.

Geissler, M., Li, K., Zhang, X.F., Clime, L., Robideau, G.P., Bilodeau, G.J. & Veres, T. 2014. Integrated air stream micromixer for performing bioanalytical assays on a plastic chip. *Lab on a Chip* 14(19): 3750–3761.

Hakansson, A, Askaner, M. & Innings, F. 2016a. Extent and mechanism of coalescence in rotor-stator mixer food-emulsion emulsification. *Journal of Food Engineering* 175: 127–135.

Hakansson, A., Chaudhry, Z., & Innings, F. 2016b. Model emulsions to study the mechanism of industrial mayonnaise emulsification. *Food and Bioproducts Processing* 98: 189–195.

Iskovich-Lototsky, R., Kots, I., Ivanchuk, Y., Ivashko, Y., Gromaszek, K., Mussabekova, A. & Kalimoldayev, M. 2019. Terms of the stability for the control valve of the hydraulic impulse drive of vibrating and vibro-impact machines. *Przeglad Elektrotechniczny* 4(19): 19–23.

Kozlov, L.G., Polishchuk, L.K., Piontkevych, O.V., Korinenko, M.P., Horbatiuk, R.M., Komada, P., Orazalieva, S. & Ussatova, O. 2019. Experimental research characteristics of counter balance valve for hydraulic drive control system of mobile machine. *Przeglad Elektrotechniczny* 95(4): 104–109.

Morgano, M.A., Milani, R.F. & Perrone, A.A.M. 2015. Determination of total mercury in sushi samples employing direct mercury analyzer. *Food Analytical Methods* 8(9): 2301–2307.

Muschiolik, G. & Dickinson, E. 2017. Double emulsions relevant to food systems: Preparation, stability, and applications. *Comprehensive Reviews in Food Science and Food Safety* 16(3): 532–555.

Obertyukh, R.R., Slabkyi, A.V., Marushchak, M.V., Koval, L.G., Baitussupov, D. & Klimek, J. 2018. Dynamic and mathematical models of the hydraulic-pulse device for deformation strengthening of materials. *Proceedings on SPIE: Photonics Applications in Astronomy, Communications, Industry, and High-Energy Physics Experiments* 10808: 108084Y.

Obertyukh, R.R., Slabkyi, A.V., Marushchak, M.V., Kobylianskyi, O.V., Wójcik, W., Yerkeldessova, G. & Oralbekov, A. 2019. Method of design calculation of a hydropulse device for strain hardening of materials. *Przegląd Elektrotechniczny R* 95(4): 65–75.

Polishchuk, L., Bilyy, O. & Kharchenko, Y. 2016. Prediction of the propagation of crack-like defects in profile elements of the boom of stack discharge conveyor. *Eastern-European Journal of Enterprise Technologies* 6(1): 44–52.

Polishchuk, L.K. & Kozlov L. G. 2018. Study of the dynamic stability of the conveyor belt adaptive drive. *Proc. SPIE, Photonics Applications in Astronomy, Communications, Industry, and High-Energy Physics Experiments* vol. 10808: 1080862.

Polishchuk, L.K., Kozlov, L.G. & Piontkevych, O.V. 2019. Study of the dynamic stability of the belt conveyor adaptive drive. *Przeglad Elektrotechniczny* 95(4): Pages 98–103.

Saravacos, G.D. 2002. *Handbook of Food Processing Equipment*. New York: Kluwer/Plenum.

Sevostyanov, I. 2013. The analysis of methods and the equipment for clearing of the damp disperse waste of food productions. *Tehnomus – New technologies and products in machine manufacturing technologies; Proc. intern. conference*, Suceava, 17–18 May 2013: 44–49.

Sevostyanov, I., Polischuk, O. & Slabkiy. 2015. A. Development and research of installations for two-component vibro-impact dewatering of food industry wastes. *Eastern-European Journal of Enterprise Technologies* 5/7(77): 40–46.

Zhu, B., Wang, X., Tan, L. & Ma Z. 2016. Investigation on flow characteristics of pump-turbine runners with large blade lean. *Journal of Fluids Engineering – Transactions of the ASME* 140(3): FE-16-1113.